A CONTINUUM DAMAGE MODEL FOR SIMULATION OF THE PROGRESSIVE FAILURE OF BRITTLE ROCKS

U. K. SINGH and P. J. DIGBY

Division of Rock Mechanics, University of Luleå, S-951 87 Luleå, Sweden

Abstract—A constitutive model is developed in which a set of continuous field variables, called damage vectors are used to describe the anisotropic response of a brittle solid due to the growth of cracks under general applied loads. The model is tested numerically by studying the response of infinitely extended solids under a number of general plane strain loading conditions.

1. INTRODUCTION

The exact description of the actual evolution of the microcrack pattern in a progressively failing brittle solid would be a difficult task. However, this process is reflected in an "average" sense by a degradation in the elastic stiffness ("softening") of the body considered due to the progressive growth and coalescence of microcracks. We may therefore quantify the process of progressive failure in a brittle solid (for example a rock) by introducing a continuous field variable called the damage, which may be regarded as a continuous measure of the state of internal degradation of the stiffness of the material considered. In such a description, the rock itself will also be regarded as a continuum on a suitable macroscopic scale whose length is large compared with a typical grain radius in the rock considered.

The concept of damage was first introduced by Kachanov (1958) for the description of creep rupture. Since that time, this concept has been used extensively to describe various types of failure processes in metals and other types of solids (see for example Lemaitre, 1986 for a review).

A formulation of an isotropic damage model (when the damage is a scalar quantity) for general three-dimensional problems is given by Dragon and Mroz (1979), and Resende and Martin (1984). However, there is strong experimental evidence to suggest that damage initiation and growth are essentially anisotropic phenomena (see for example Paterson, 1978). A number of more general anisotropic damage models were therefore proposed. Thus, Davison and Stevens (1973) regarded the damage in a brittle material as a vector quantity whose magnitude and direction were related in an average sense to a large number of cracks in the neighbourhood of the point considered. The damage vector was taken as an internal state variable. Finally, to complete the model, a simplified damage accumulation function relating the damage growth to the current stress and damage was proposed.

Krajcinovic and Fonseka (1981) in their elegant model, used a similar approach. However, unlike the previous case, the damage growth law was not formulated directly. They related the damage growth in different directions to increments in strain through a set of damage surfaces $^{z}F(D, \varepsilon)$ $(z = 1, 2, \ldots, n)$ in deformation space, associated with the damage vector in different directions. Their development of a damage growth model depends on the existence of a normality rule in which a damage increment is normal to the corresponding damage surface. This in turn depends on the assumption of "path independence in the small" (see for example Singh, 1986). Here, the work done in producing a small change in damage is independent of the path used in deformation space in passing between the two damage states. A very closely related derivation of an analogous normality rule in plasticity has been presented by Dougill (1975), by using the concept of path independence in the small as an initial postulate in the mathematical theory of plasticity. The model described in this paper for the description of damage growth, most closely resembles the one formulated by Krajcinovic and Fonseka (1981). However, there are a number of

important differences, both in the formulation of our model and in the problems considered. Thus, unlike the damage growth model constructed by Krajcinovic and Fonseka (1981), our damage growth model does not depend on any assumption concerning path independence in the small. Motivated by the work of Griffith and Murrell, described in Jaeger and Cook (1979), we have taken our damage surface in strain space to be parabolic rather than hyperbolic as was the case in Krajcinovic and Fonseka's work. In the present paper, we also formulate components of the stiffness tensor in an approximate manner directly from micro-mechanical considerations. We apply our model to the study of a number of plane strain problems in which an infinitely extended brittle solid undergoes progressive failure under general biaxial loading.

2. SOME PRELIMINARY DEFINITIONS

2.1. *Sign convention*

Throughout this work, we adopt the convention that tensile stresses and strains are positive and compressive stresses and strains are negative.

2.2. *The damage variables*

The direction of a damage vector ^{x}D ($x = 1, 2, \ldots, n$) is defined by the unit vector $\hat{x}$ normal to a given set of flat, penny-shaped cracks. In a given direction $\hat{x}$, all growing cracks remain penny shaped and have the same radius ^{x}a. The crack radii for cracks in different directions need not, however, be the same. We also suppose that the damage growth in a given direction is independent of the damage growth in other directions. Also, any number of damage vectors ^{x}D may simultaneously exist at a given point in the material considered. The magnitude of the damage vector ^{x}D in a particular direction $\hat{x}$ is defined as follows:

$$^{x}D = \frac{^{x}N}{V}\, ^{x}v \quad \text{(no summation over } x!), \quad x = 1, 2, \ldots, n. \tag{1}$$

Here ^{x}N is the total number of penny-shaped cracks all of radius ^{x}a in the direction $\hat{x}$, all contained within a spherical sample volume V whose radius R is much larger than any crack radius ^{x}a. ^{x}v is the volume of a sphere of radius ^{x}a.

We also define the effective damage vector, $^{\beta}\dot{D}$ in a particular direction $\hat{\beta}$, due to the damage vectors ^{x}D ($x = 1, 2, \ldots, n$) in other directions $\hat{x}$ by the equation

$$^{\beta}\dot{D} = \sum_{x=1}^{n} {}^{x}D|\cos{}^{x}\theta|. \tag{2}$$

In eqn (2), $^{x}\theta$ is the angle between the normal to a selected "effective" damage plane and the normal $\hat{x}$ to an actual damage plane. We note here that we may have an "effective" damage in a particular direction without having an actual damage in this direction.

2.3. *Coordinate axes*

0123 (with unit vectors $\hat{e}_{1}, \hat{e}_{2}, \hat{e}_{3}$ directed along 01, 02, 03) denotes a fixed set of right-handed orthogonal Cartesian axes (called the global axes) embedded in the rock we are considering (Fig. 1). 03′ (in direction $\hat{x}$) denotes the normal to a penny-shaped crack (center 0) in the solid we are considering. The 01′ axis is now defined by the intersection of the crack (damage) plane with the plane 102. The 02′ axis is then defined so that axes 01′2′3′ with unit vectors $\hat{e}'_{1}, \hat{e}'_{2}, \hat{e}'_{3}$ directed along 01′, 02′, 03′, respectively also form a right-handed set of orthogonal axes. These are called the local axes.

Throughout this paper tensor components of type $\sigma_{ij}, \varepsilon_{ij}$ and K_{ijmn} ($i, j, m, n = 1, 2, 3$) denote the Cartesian components of the stress, strain and elastic stiffness tensor σ, ε and K, respectively, referred to the gobal axes. Referred to this set of axes, the unit vector $\hat{x}$ also has the components $\hat{x} = (n_{1}, n_{2}, n_{3})$.
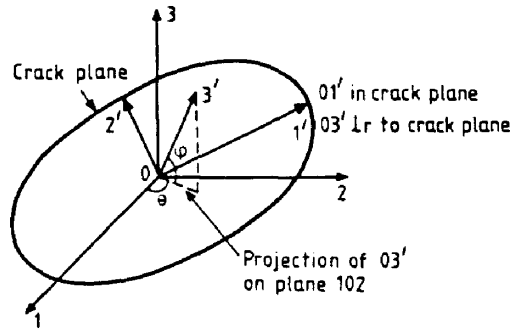
Fig. 1. A penny-shaped crack with coordinate systems.

2.4. The strain traction vector defined on a damage plane

In later sections of this paper, we will find it convenient to define the ith component of the strain traction vector ε_R acting on a crack plane (damage plane) with unit normal $\hat{x}$, by the equation

$$(\varepsilon_R)_i = \varepsilon_{ji} n_j \quad (i, j = 1, 2, 3). \tag{3}$$

The magnitude of ε_R is given by

$$\varepsilon_R = (\varepsilon_{ji} \varepsilon_{ki} n_j n_k)^{1/2}. \tag{4}$$

The component of ε_R in the direction of $\hat{x}$ is given by

$$\varepsilon_N = \varepsilon_{ji} n_i n_j. \tag{5}$$

The component of ε_R in the damage plane (crack plane) is then given by

$$\varepsilon_T = (\varepsilon_{ji} \varepsilon_{ki} n_j n_k)^{1/2} (\delta_{il} - n_i n_l)^{1/2} \tag{6}$$

where δ_{il} is the usual Kroneker delta symbol.

2.5. The effective stiffness tensor

Referred to our fixed axes, we write components of the fourth order effective elastic stiffness tensor, corresponding to states of damage ^xD as functions of $^1D, ^2D, \ldots, ^nD$ in the abbreviated form

$$\bar{K}_{ijmn} = K_{ijmn}(D). \tag{7}$$

For a material in the undamaged state, we define

$$^xD = 0 \quad (x = 1, 2, \ldots, n) \quad \text{and} \quad \bar{K}_{ijmn} = K_{ijmn} \tag{8}$$

where K_{ijmn} refer to the components of the elastic stiffness tensor of the initially undamaged elastically isotropic, homogeneous material. Grady and Kipp (1980), in their scalar damage model, scaled the entire failure state of the material so that the damage always lies between zero and unity. In our model, however, no advantage is gained by performing this exercise, so that the magnitude of any damage vector can exceed unity.

3. THE CONTINUUM DAMAGE MODEL

3.1. The constitutive relations

Here, the set of damage vectors ^xD ($x = 1, 2, \ldots, n$) defined in Section 2.1 is taken to be a set of internal variables describing the state of the material considered. It is supposed

that the process described by this set of variables is the only source of irreversible behaviour in the material considered. The damage in the material is defined to be irreversible in the sense that the initial, undamaged state cannot be recovered on unloading. We also suppose here that the unloading is purely elastic, and that no further damage occurs during any unloading process.

We have followed the formulation of constitutive equations based on thermodynamics with internal variables. This has been studied extensively and in considerable detail by Rice (1971, 1975), Kestin and Bataille (1977), Krajcinovic and Fonseka (1981) and Singh (1986). We therefore present only the final constitutive equations. We might mention, however, that the existence of thermodynamic potentials for deformations in which the damage vectors $^{\alpha}D$ ($\alpha = 1, 2, \ldots, n$) are held fixed (Rice, 1975), is perhaps the most important basic assumption used in the work cited above. Expressed in the form of a total stress–strain relation, our required constitutive equations may be written in the form

$$\sigma_{ij} = \bar{K}_{ijmn}(D)\varepsilon_{mn} \quad \text{for a given } fixed \ ^{\alpha}D \quad (\alpha = 1, 2, \ldots, n). \tag{9}$$

The components of the effective elastic stiffness tensor in eqns (9) above satisfy the following symmetries:

$$\bar{K}_{ijmn} = \bar{K}_{jimn} = \bar{K}_{ijnm} = \bar{K}_{mnij}. \tag{10}$$

In eqns (9) and throughout this paper, thermal effects are neglected.

3.2. The damage surface

Damage surfaces in the continuum damage theories of brittle rocks are intended to play a similar role as yield surfaces in the hardening theory of plasticity. However, following Krajcinovic and Fonseka (1981), these surfaces are always formulated in strain space. In particular, the equations of each damage surface used in this paper will be written in terms of the effective damage (eqn (2)) and the components of the strain traction vector normal to and in the damage plane, $^{\alpha}\varepsilon_N$ and $^{\alpha}\varepsilon_T$, respectively (see eqns (4) and (5)). Thus, we write the equations for the set of all damage surfaces (all have the same functional form) in terms of a scalar function F as follows.

$$F(^{\alpha}\varepsilon_N, ^{\alpha}\varepsilon_T, ^{\alpha}\dot{D}) = 0 \quad (\alpha = 1, 2, \ldots, n). \tag{11}$$

Krajcinovic and Fonseka (1981) proposed a hyperbolic damage surface for concrete and rock. However, as mentioned in the introduction to this paper, we have selected an alternative form for F. Thus, motivated by the work of Mohr, Griffith and Murrell (described in Jaeger and Cook, 1979) we suppose that in ε_N, ε_T space each damage surface for a brittle rock is a parabola whose equation may be written in the form

$$F(^{\alpha}\varepsilon_N, ^{\alpha}\varepsilon_T, ^{\alpha}\dot{D}) = F(^{\alpha}\varepsilon) - Y(^{\alpha}\dot{D}) = 0 \tag{12}$$

where

$$F(^{\alpha}\varepsilon_N, ^{\alpha}\varepsilon_T) = ^{\alpha}\varepsilon_N + A_1^{\alpha}\varepsilon_T^2 \tag{13}$$

$$Y(^{\alpha}\dot{D}) = A_2^{\alpha}\dot{D}^{1/3} + A_3. \tag{14}$$

$A_i \geq 0$ ($i = 1, 2, 3$) are material parameters which must be determined experimentally. The damage surfaces we use (eqns (12)–(14)) have the following features:

(i) The damage surface is symmetric with respect to the sign of ε_T, that is the damage can grow in shear for "negative" as well as for "positive values" of the in-plane components of the strain traction vector ε_R.

(ii) If ε_r is zero, the damage can grow only when ε_N has a positive value, that is, in the absence of shear, cracks can grow in tension only. This is consistent with the assumption we have made in Section 3.1 of this paper. From eqns (12) and (13), the condition for crack (damage) growth in pure tension is

$$^2\varepsilon_N > A_2^{\frac{1}{2}}\dot{D}^{1/3} + A_3.$$ (15)

(iii) Analogously to the behaviour of a yield surface in the theory of hardening in plasticity, we see from eqns (13), (14) that as the effective damage $^2\dot{D}$ increases, the corresponding damage surface expands in strain space.

3.3. Damage growth initiation

In this paper, we study the process of progressive failure in a brittle rock subjected to quasi-static applied loading rates. In a body failing under loads applied in a given direction and applied at sufficiently low rates, it is generally accepted that only a small number of critically oriented cracks participate in the fracture process; see for example work of Griffith and Murrell in Jaeger and Cook (1979) and Grady and Kipp (1980). Following these ideas, we therefore suppose that further constraints must be imposed on eqns (12)–(14) to restrict the number of possible damage growth directions at any given load increment.

We define our damage growth direction by requiring that the conditions for $F(^2\varepsilon_N, {}^2\varepsilon_r)$ (in eqns (13) and (14)) to be a maximum and the inequality

$$F(^2\varepsilon_N, {}^2\varepsilon_r) > Y(^2\dot{D})$$ (16)

are simultaneously satisfied. We have determined the directions of the unit normal $\hat{x} = (n_1, n_2, n_3)$ to the damage plane for which the function $F(^2\varepsilon_N, {}^2\varepsilon_r)$ in eqns (13) and (14) takes maximum values by using the method of Lagrange Multipliers. These directions were determined for a body under general triaxial loading conditions (and not just for plane strain loading conditions). The following results were obtained.

(i) For $A_1(\varepsilon_1 - \varepsilon_3) \leqslant 1$:

$$\max F(^2\varepsilon_N, {}^2\varepsilon_r) = \varepsilon_1 \quad \text{with} \quad \hat{x} = (1, 0, 0).$$ (17a)

That is, $\hat{x}$ is parallel to the direction of the maximum applied principal strain ε_1.

(ii) For $A_1(\varepsilon_1 - \varepsilon_3) > 1$:
Here,

$$\max F(^2\varepsilon_N, {}^2\varepsilon_r) = \tfrac{1}{2}(\varepsilon_1 + \varepsilon_3) + \frac{A_1}{4}(\varepsilon_1 - \varepsilon_3)^2 + \frac{1}{4A_1}$$

with

$$\hat{x} = (\cos \xi, 0, \sin \xi) \quad \text{and} \quad (\cos (\pi - \xi), 0, \sin (\pi - \xi)) \quad \left\} \right. \quad (17b)$$

where

$$\xi = \tfrac{1}{2}\cos^{-1}\left(\frac{1}{A_1(\varepsilon_1 - \varepsilon_3)}\right).$$

Here, we see that damage growth can occur in two conjugate directions.

The maximum value of $F(^2\varepsilon_N, {}^2\varepsilon_r)$ is therefore independent of the intermediate applied principal strain, ε_2, as is the damage. An analogous result in stress space was obtained for triaxially stressed brittle solids by Murrell and Digby (1970). This was to be expected, since Murrell and Digby (1970) extended the Griffith approach for triaxially stressed brittle solids, to derive a parabolic failure envelope in stress space.

3.4. Conjugate and non-conjugate damage growth

In our computations (see Section 6) the damage initiation condition (16) is actually checked numerically for damage growth in the potentially active direction by checking whether

$$\max F(^{\alpha}\varepsilon_N^{r+1}, {}^{\alpha}\varepsilon_T^{r+1}) > Y(^{\alpha}\dot{D}^r) \tag{18}$$

where $^{\alpha}\varepsilon_N^{r+1}$, $^{\alpha}\varepsilon_T^{r+1}$ refer to components of the strain traction vector computed at the $(r+1)$th load increment and $^{\alpha}D^r$ refers to the effective damage computed from eqn (2) at the preceding rth load increment.

In case (ii) (eqns (17b)), the normals for which $F(^{\alpha}\varepsilon_N, {}^{\alpha}\varepsilon_T)$ takes maximum values are directed symmetrically about the axis of the minimum principal strain ε_3. These normals will then define two possible planes in which the damage can first grow. Whenever the condition (18) is satisfied, two cases must then be considered.

(i) *Non-conjugate damage growth*. Here, the normal to the damage plane at the preceding rth load increment is not symmetric with respect to the calculated directions of α (eqns (17b)) at the $(r+1)$th load increment, but makes angles $^1\theta$ and $^2\theta$ with these directions (see Fig. 2) where $^2\theta < {}^1\theta$, say. We then have at the rth load increment (from eqn (2)),

$$^2\dot{D} > {}^1\dot{D} \quad \text{and so} \quad Y(^2\dot{D}) > Y(^1\dot{D}) \tag{19}$$

(see eqns (14)). In this case, damage growth is permitted only in the damage plane normal to the direction $\alpha = 2$ for which $Y(\dot{D})$ is largest. We then have the case of non-conjugate damage growth, and we take

$$\Delta^2 D = \Delta^2 \dot{D},$$

since in this case $\Delta^1 \dot{D} = 0$.

(ii) *Conjugate damage growth*. Here, the normal to the damage plane at the rth load increment is symmetric with respect to the potential damage growth directions computed at the $(r+1)$th load increment. We then have $^1\theta = {}^2\theta = \theta/2$ say, and so, from eqns (2),

$$^2\dot{D} = D|\cos {}^1\theta| = D|\cos {}^2\theta| = D|\cos (\theta/2)| = {}^1\dot{D}, \tag{20}$$

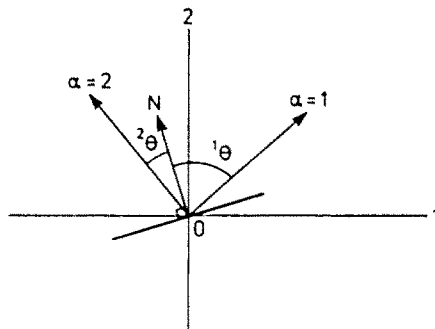that is, $Y(^1\dot{D}) = Y(^2\dot{D})$.

Fig. 2. $\alpha = 1$ and 2 are normal to the potential damage planes. $0N$ is normal to the damage plane at the preceding load increment.

Here, we have conjugate damage growth along the two damage planes normal to the directions $x = 1$ and $x = 2$. Since

$$\Delta^1 D = \Delta^2 D = \Delta D \neq 0,$$

$$\Delta^2 \dot{D} = \Delta^2 D + \Delta^1 D |\cos \theta| = \Delta^2 D(1 + |\cos \theta|) = \Delta^1 \dot{D}.$$

Therefore,

$$\Delta^2 D = \Delta^2 \dot{D}/b \tag{21}$$

where $b = (1 + |\cos \theta|)$.

3.5. Summary of the damage growth model

We may now summarize our damage growth model as follows. ε_{r+1} denotes the strain tensor at $(r+1)$th load increment. At this load increment we first calculate the directions $\dot{x} = (n_1, n_2, n_3)$ for which the function $F(^x\varepsilon_N^{r+1}, {}^x\varepsilon_T^{r+1})$ (eqns (12)–(14)) is a maximum. As explained in the preceding section, this defines one, or at most two potentially active conjugate damage growth directions at the $(r+1)$th load increment. From eqn (2), we now compute the effective damage (in these calculated directions) at the preceding rth load increment, that is we compute

$$^x\dot{D}^r = {}^xD^r + \sum_{\beta=2}^{n} {}^\beta D^r |\cos {}^\beta\theta|. \tag{22}$$

For these computed, potentially active damage directions, we then calculate $Y({}^x\dot{D}^r)$ from eqn (14).

We then check the damage initiation condition (18). If this condition is satisfied, we then compute the new effective damage, at the $(r+1)$th load increment, from eqns (12)–(14), that is

$$^x\dot{D}^{(r+1)} = x^3 \quad \text{where} \quad x = ({}^x\varepsilon_N^{r+1} + A_1({}^x\varepsilon_T^{r+1})^2 - A_3)/A_2. \tag{23}$$

We then obtain

$$\Delta^x\dot{D} = {}^x\dot{D}^{r+1} - {}^x\dot{D}^r$$

and hence either

(i) $^xD^{r+1} = {}^xD^r + \Delta^x\dot{D}$

for non-conjugate damage growth, or

(ii) $^xD^{r+1} = {}^xD^r + \Delta^x\dot{D}/b$

for conjugate damage growth, where $b = 1 + |\cos \theta|$ and θ is the angle between conjugate damage planes.

The empirically constructed yield function $Y(\dot{D})$ defined earlier by eqns (14) leads to computations in which very sharp stress drops can be encountered. To circumvent this difficulty in the numerical computations, we have therefore modified our yield function (eqns (12)-(14)) as follows:

$$\left.\begin{aligned}
F(\varepsilon) &= \varepsilon_N + A_1\varepsilon_T^2 \\
Y(\dot{D}) &= A_2\dot{D}^{1/3} + A_3 \\
\dot{D} &= \frac{(\varepsilon_N + A_1\varepsilon_T^2 - A_3)^3}{A_2^3} = x^3
\end{aligned}\right\} \quad \text{for } x < \sqrt{(2/3)} \tag{24a}$$

$$F(\varepsilon) = \varepsilon_V + A_1 \varepsilon_T^2.$$

$$\dot{Y}(\dot{D}) = \frac{A_2}{2}(\dot{D} + 1.0886621) + A_3$$

$$\dot{D} = 2\frac{(\varepsilon_V + A_1 \varepsilon_T^2 - A_3)}{A_2} - 1.0886621$$

$$= 2x - 1.0886621.$$

for $x \geqslant \sqrt{(2/3)}$ \quad (24b)

We note that the graphs for the function $\dot{D}$ as a function of x defined by eqns (24) above join continuously and smoothly at $x = \sqrt{(2/3)}$. We note that, unlike the damage growth model constructed by Krajcinovic and Fonseka (1981), our damage growth model does not depend on any assumption concerning path independence in the small.

4. THE EFFECTIVE ELASTIC COMPLIANCE OF A DAMAGED BRITTLE ROCK

We now complete the formulation of our continuum damage model by describing the approximate calculation of the effective elastic compliance of a cracked elastic solid.

The elastic response of a cracked solid may be written in the form

$$\varepsilon_{ij} = \bar{C}_{ijmn}\sigma_{mn} \quad (i, j, m, n = 1, 2, 3) \tag{25}$$

where $\bar{C}_{ijmn}$ denote the components of the effective compliance tensor of the cracked (damaged) solid we are considering. As indicated in the introduction of this paper, we derive approximate explicit expressions for the compliance components in terms of the crack concentration based on microstructural considerations. Now, in general, the effective elastic compliance of a cracked elastic solid should be larger than the initial compliance of the uncracked solid. Following Horii and Nemat-Nasser (1983), the effective elastic compliance of a cracked solid is therefore written in the form

$$\bar{C}_{ijmn} = C_{ijmn} + H_{ijmn} \quad (i, j, m, n = 1, 2, 3) \tag{26}$$

where C is the elastic compliance tensor for the uncracked solid (assumed elastically isotropic and homogeneous with Young's modulus E and Poisson's ratio v). H is the contribution to the effective elastic compliance $\bar{C}$ due to all the cracks. Suppose now that S denotes the contribution to H from a single crack. Following Horii and Nemat-Nasser (1983), we then obtain the following components of S referred to the local axes $01'2'3'$ (see Section 2.2).

$$S'_{3333} = \frac{16(1-v^2)}{3E}a^3 f_n$$

$$S'_{1313} = S'_{2323} = \frac{8(1-v^2)}{3E(2-v)}a^3 f_s, \quad \text{and}$$

all other components S'_{ijmn} are zero.

\quad (27)

Consistent with our assumptions in Section 2.2 regarding the independence of damage growth in different directions, it is assumed in the derivation of these results (see Horii and Nemat-Nasser, 1983), that the effect of crack interaction may be ignored.

Now let σ_N $(= \sigma_{ij}n_i n_j)$ denote the component of stress normal to the plane of a given crack and σ_{Nc} (<0) be the critical normal compressive stress at which the crack may be considered to be closed. The functions f_n and f_s are then defined as follows.

$$f_n = f_t = 1 \qquad \text{for } \sigma_N/\sigma_{Nc} \leqslant 0, \text{ i.e. when } \sigma_N \text{ is tensile and the cracks are open.}$$

$$f_n = (1 - \sigma_N/\sigma_{Nc})^2 \qquad \text{for } 0 < \sigma_N/\sigma_{Nc} < 1, \text{ i.e. when } \sigma_N \text{ is compressive and the cracks are partially closed.}$$

$$= 0 \qquad \text{for } \sigma_N/\sigma_{Nc} \geqslant 1, \text{ i.e. when } \sigma_N \text{ is compressive and the cracks are completely closed.} \tag{28}$$

$$f_t = (1 - \sigma_N/\sigma_{Nc}) \qquad \text{for } 0 < \sigma_N/\sigma_{Nc} < 0.8, \text{ i.e. when } \sigma_N \text{ is compressive and the cracks are partially closed.}$$

$$= 0.2 \qquad \text{for } \sigma_N/\sigma_{Nc} \geqslant 0.8, \text{ i.e. when } \sigma_N \text{ is compressive and the cracks are either almost or completely closed.} \tag{29}$$

From eqns (27) we see that referred to the local axes, S'_{3333}, S'_{1313} and S'_{2323} are the only non-zero components of the compliance tensor S, and hence a penny-shaped crack affects the overall response only in a direction normal to the crack plane. If now there are n cracks per unit volume oriented parallel to this crack, we then obtain from eqns (1), (27), (28)

$$H'_{3333} = \frac{16(1 - v^2)}{3E} {}^3D f_n,$$

$$H'_{1313} = H'_{2323} = \frac{8(1 - v^2)}{3E(2 - v)} {}^3D f_t, \quad \text{and} \tag{30}$$

all other components H'_{ijmn} are zero.

Hence, turning now to the case in which damage planes exist simultaneously in several directions in the material, we obtain from eqns (26) and (30),

$$\bar{C}_{ijmn} = C_{ijmn} + \sum_{x=1}^{n} (T_{pi} T_{qj} T_{rm} T_{sn} H'_{pqrs}) \tag{31}$$

for the components of the effective compliance tensor $\bar{C}$ referred to the global axes. In eqns (31) T_{ij} denote the components of the transformation tensor T from the global to the local axes, that is

$$e'_i = T_{ij} e_j. \tag{32}$$

The summation sign in eqn (31) denotes the summation over all possible orientations of the axes $01'2'3'$ relative to the global axes 0123 (that is an orientation average). The corresponding components $\bar{K}_{ijmn}$ of the effective stiffness tensor may be calculated by taking the inverse of the effective compliance tensor $\bar{C}$ given by eqns (26), (31).

5. PARAMETERS USED IN THE MATERIAL MODEL

The parameters used in our material model may be divided into two groups as follows.

(i) Effective elastic compliance $\bar{C}$:
E, Young's modulus of elasticity for the intact rock ;
v, Poisson's ratio for the intact rock ;
σ_{Nc}, the critical compressive stress for crack closure.

(ii) Damage surface and damage growth (eqns (12)-(14)):
A_1, a measure of the damage initiation in pure shear, that is in the absence of tensile strain for a given value of A_3 ;
A_2, controls the damage growth rate for given values of A_1 and A_3 ;
A_3, critical extension strain at which damage initiates in a rock specimen in the absence of a shear strain ;
D_0, the initial damage, assumed isotropic.

In this section, we describe methods by which the values of parameters used in our material model (listed above) might be determined.

E and v may be determined by standard uniaxial or triaxial laboratory tests on intact rock specimens (see for example Lama and Vutukuri, 1978). E and v are the Young's modulus and Poisson's ratio respectively for an intact rock loaded to the point where damage growth (non-linear constitutive behaviour) may first be detected. Digby and Murrell (1976) have given a general expression for the compressive stress required to close an ellipsoidal crack (with axes $a \geqslant b \gg c$) in a triaxially stressed solid. For the special case of a penny-shaped crack, their result is

$$\sigma_{Nc} = -\frac{\pi E}{4(1 - v^2)} \left(\frac{c}{b}\right).$$ (33)

This is similar to Walsh's (1965) result for a body loaded under plane strain conditions. Substituting $E = 30 \times 10^9$ Pa, $v = 0.2$ (the values of E and v for Stripa granite listed in Table 1), and $(c/b) = 0.0001$ (very flat crack) in eqn (33), we get $\sigma_{Nc} \approx -2.5 \times 10^6$ Pa. We note that the crack closure stress should change with the crack aspect ratio. However, in our model, we suppose that σ_{Nc} is a constant (calculated for a very flat crack) for simplicity.

The parameter A_1 may be determined from a uniaxial tension test. We might detect the critical extension strain for which a change of slope in the load–deformation curve occurs or the initiation of acoustic emission from the sample just before the initiation of failure.

To determine the parameter A_1, we first write

$$A_1 = A_1/\varepsilon_{Tc}^2$$ (34)

from eqns (12)–(14) with $\varepsilon_N = 0$, $D \approx 0$. Here, ε_{Tc} is the critical shear strain at which damage (crack) growth in pure shear initiates. It is very difficult to obtain reliable measurements of the shear strain (see for example Shahidi *et al.*, 1986). Otherwise, the critical shear strain ε_{Tc} could be determined by methods analogous to those used for the determination of the parameter A_1. However, one may first obtain a lower bound for the critical shear strain ε_{Tc} by observing that an intact brittle rock is stronger in shear than in tension. Thus we can write

$$\varepsilon_{Tc} = \chi A_1, \quad \text{for } \chi > 1.$$ (35)

We could then use eqns (34), (35) to estimate the parameter A_1,

$$A_1 = 1/\chi^2 A_1$$ (36)

by using some reasonable value for χ ($= 4$, say). We could then simulate numerically a uniaxial compression test and check whether the calculated value of A_1 is a reasonable value for the uniaxial compressive strength of the specimen. Here, we can also use the observation from eqns (17a) and (17b) that the magnitude of $A_1(\varepsilon_1 - \varepsilon_3)$ also controls the type of damage (crack) growth under given applied load conditions. It is the growth of an inclined damage plane which leads to the peak load in compression.

The simplest test for determination of the parameter A_2, controlling the rate of damage growth, might again be a uniaxial tension test where progressive failure is controlled by the growth of a single damage plane normal to the applied load direction. We may then estimate the damage in this test by measuring the effective elastic compliance of the test specimen. This may be calculated from the slope of the unloading curve. The effective compliance considered is related to the damage through eqns (30) and (31). By specializing these equations to the case of a single damage plane we then obtain

$$\frac{\bar{E}}{E} = \left\{1 + \frac{16(1 - v^2)}{3} D\right\}^{-1}$$ (37)

Table 1. Material and numerical parameters obtained from the uniaxial tension tests

Parameter	Value
E	30.0×10^9 Pa
v	0.2
σ_{vc}	-0.5×10^6 Pa
A_1	312.5
A_2	1.15×10^{-3}
A_3	0.20×10^{-3}
D_0	1.0×10^{-5}

Modified damage growth law given by eqns (24a) and (24b)

where $\bar{E}$ is the effective Young's modulus in the applied load direction. Thus, having determined $\bar{E}$, E and A_1 as described above, D may be calculated from eqn (37) and hence the value of A_2 determined.

In the application of our model to the numerical computations to be described in the next section, the numerical values of the material parameters used in the computations are listed in Table 1. These were obtained from uniaxial tension and simple shear tests on samples of a grey, medium-grained granite from the Stripa mine in central Sweden (see Shahidi *et al.*, 1986 for further details).

6. NUMERICAL SIMULATIONS AND RESULTS OBTAINED

In the application of our damage model to the study of progressive failure, we will always restrict our attention to the case in which the body considered is loaded under plane strain conditions. In this section we describe a number of idealized problems. These were used to verify that physically satisfactory results could be obtained from our model before it was to be implemented into a finite element computer code. Thus we describe the results obtained from our model when we study the progressive failure process in an infinitely extended body under different conditions of loading and initial damage. Here, since the body is infinitely extended, we suppose that the damage in any given direction is uniformly distributed throughout the body, and further, therefore, that localization effects need not be considered for this group of idealized problems.

6.1. *Plane strain case of the damage material model*

We consider the two-dimensional coordinate system shown in Fig. 3. The axis 03, normal to the plane 102, always coincides with the directions of principal stress and strain. All field quantities are independent of the direction 03. For the plane strain problems considered in this work we make the usual assumptions:

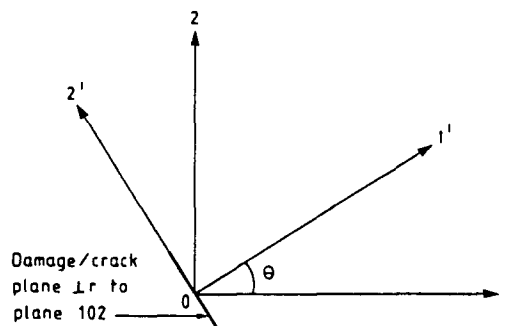$$\varepsilon_{33} = \varepsilon_{13} = \varepsilon_{23} = 0. \tag{38}$$

Fig. 3. Two-dimensional coordinate system. Plane 102 is a two-dimensional plane. Axis 01' denotes the damage direction.

We follow the notation used in Section 2.3, but now with the local axes renumbered for convenience. Thus, axis 01' (Fig. 3) is taken to be normal to the damage (crack) plane and 02' lies in the damage plane.

6.2. Numerical results

The behaviour of our constitutive model for a body loaded under plane strain conditions has been studied by specifying strain increments as load increments along the 01 axis and a constant stress along the 02 axis. An IBM PS 2 model 60 computer was used in all of the computations described in this section. The numerical results are obtained from the values of the material parameters listed in Table 1.

The curves 1, 2 and 3 in Fig. 4 illustrate the behaviour of our constitutive model for an infinitely extended body loaded in tension along the 01 axis but with no confining stress applied along the 02 axis, i.e. $\sigma_2 = 0$. The set of curves 1 (corresponding to a small initial damage $D_0 = 1 \times 10^{-5}$, uniformly and isotropically distributed) is very similar to those described in Singh (1986). The set of curves 2 and 3 correspond to initial damages of magnitudes 0.5 and 2.0, respectively, with the normal to all the initial damage planes inclined at 70 degrees to the 01 axis in both these cases. The pre-failure slopes of curves 2 and 3 in Fig. 4(a) are smaller than those of curve 1. Here, the initial finite damage in the case of curves 2 and 3 has reduced the effective Young's modulus along the applied load direction 01. The unloading–reloading curve 2 illustrates that the effective Young's modulus and Poisson's ratio decreases with an increase in damage (Fig. 4(a) and (b)). During unloading from a damaged state and reloading to the same state, the total damage does not change (Fig. 4(d)), and in this case, the behaviour is elastic (Fig. (4(a), (b) and (c)). We get a shear strain, as shown in Fig. 4(c), in the coordinate system 102 for finite initial damages inclined to the 01 axis. In this case, the principal stress and principal strain axes do not coincide.
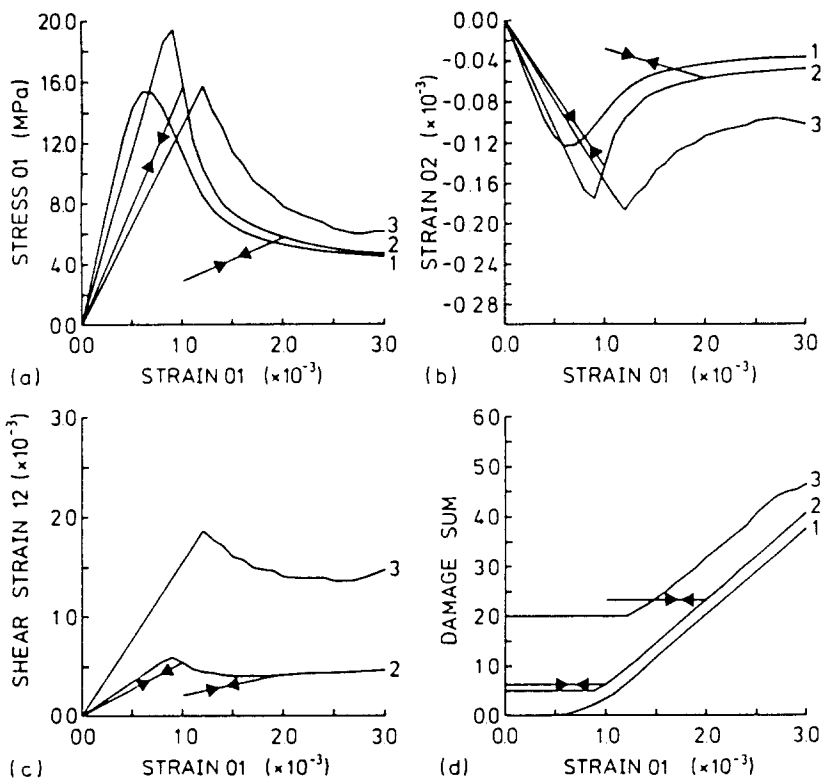

Fig. 4. Numerical tension experiment. Curve 1 is for isotropic small initial damage ($D_0 = 1 \times 10^{-5}$).
Curve 2 for damage 0.5. Normal to this initial damage plane makes an angle of 70° to the axis 01.
Curve 3 for damage 2.0. Normal to this initial damage plane makes an angle of 70° to the axis 01.
Confining stress σ_2 is zero for all the curves.

Since the magnitude of the initial damage for curve 1 is smaller than that for the case of curves 2 and 3, we might have expected that the peak stress for curve 1 in Fig. 4(a) would have been larger than that for curves 2 and 3. This discrepancy is due to the fact that there is a non-zero shear strain in the case of curves 2 and 3, and the way we calculate the potential damage growth directions from eqns (17). However, curve 3 has a lower peak-stress than curve 2, as expected.

Numerical experiments were performed for an infinitely extended body loaded under increasing compressive stress applied along the 01 axis. These were performed at three levels of constant confining stresses, $\sigma_2 = 0$, -5 and -10 MPa corresponding to curves 1, 2 and 3, respectively in Figs 5–7.

Figure 5 illustrates numerical results from the plane strain compression test where the condition for conjugate damage growth is satisfied. We have specified a small initial isotropic damage D_0 to obtain conjugate damage growth during the proportional load increment. We observe an increase in peak-load with increasing confining stresses (Fig. 5(a)). Damage growth begins before the peak-load is reached, as shown in Fig. 5(c). However, the peak-load occurs at a relatively small value of the damage and at a relatively small increase in compliance. Some damage planes, whose normals were almost perpendicular to the applied load axis 01 were observed. At the peak load, conjugate damage planes whose normals were inclined at angles of 71 and 109 degrees to the 01 axis were active. As loading continues beyond the post-peak region, the damage grows rapidly (Fig. 5(c)) and the growth of damage planes whose normals make increasing angles to the applied load axis 01 also occurs. It is important to note how the strain 01–strain 02 curves in Fig. 5(b) illustrate departure from linearity in behaviour near the peak-load. The strain 02 suddenly increases quite rapidly in the post-failure regime. This behaviour has been observed in laboratory tests on brittle rocks (Paterson, 1978). In this case of conjugate damage growth, we could
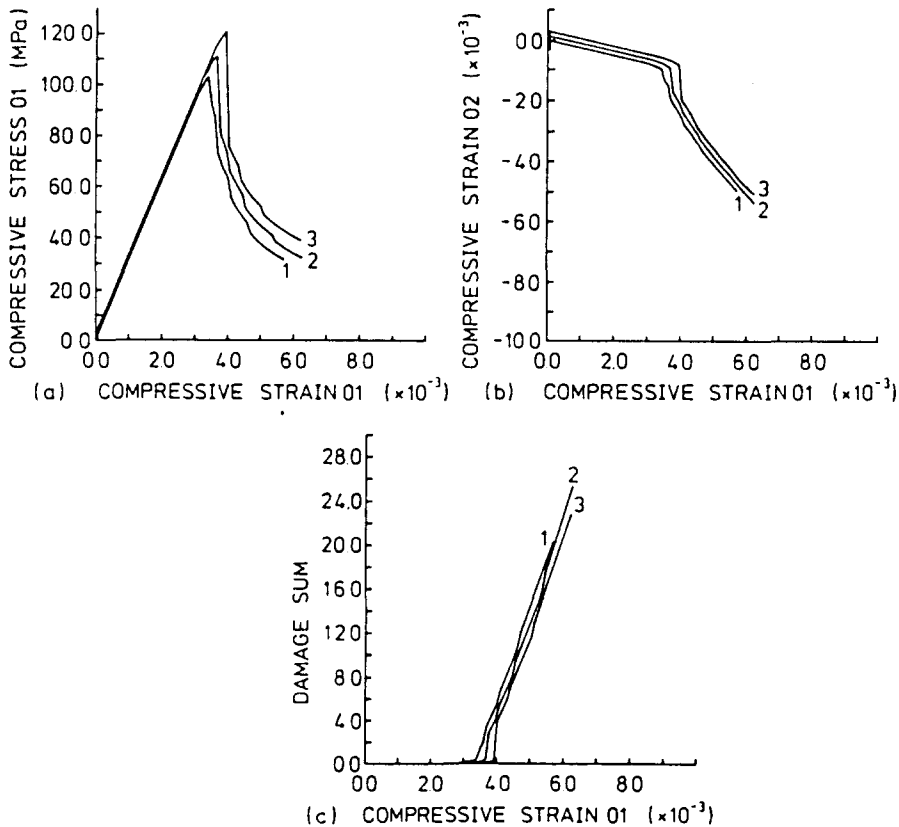

Fig. 5. Numerical compression experiment, with small initial isotropic damage ($D_0 = 1 \times 10^{-3}$), and conjugate damage growth. Curve 1 is for confining pressure σ_2 of 0 MPa; curve 2 for -5 MPa; curve 3 for -10 MPa.
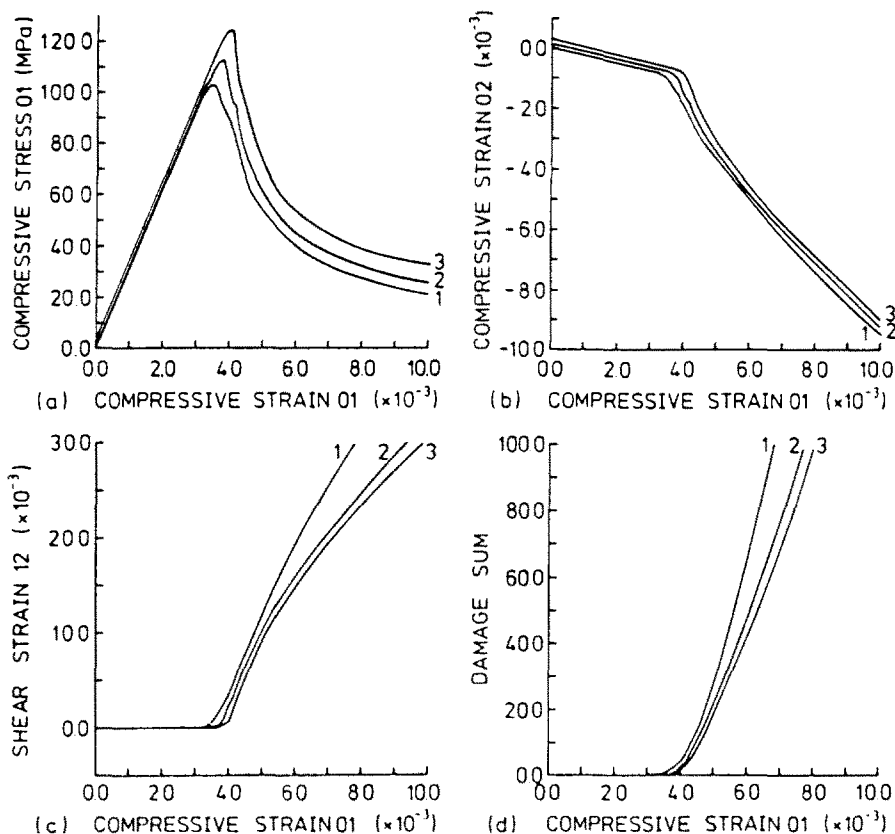
Fig. 6. Numerical compression experiment with initial damage 0.005. Normal to this initial damage plane makes an angle of 70 to the 01 axis. Non-conjugate damage growth. Curve 1 is for confining pressure σ_2 of 0 MPa; curve 2 for −5 MPa; curve 3 for −10 MPa.

not continue our numerical experiments beyond a level of strain 01 = 6 × 10^{-3} because the specified computer storage space for the damages and their directions was exhausted.

The condition for conjugate damage growth is usually violated in practice, for example, due to the presence of a finite initial damage (cracks) in a particular direction and a change in load direction after the initial damage growth. To study the response of the constitutive model in the case of non-conjugate damage growth, we introduced a set of initial damage planes whose normals were all inclined at an angle of 70 degrees to the applied load axis 01. Here, the magnitude of the initial damage was 0.005. The results are presented in Fig. 6. Here, all the curves show trends similar to those shown in Fig. 5 for the conjugate damage growth case. However, the number of damage directions is smaller than the number for the conjugate damage growth case and the components $\bar{C}_{11}$ and $\bar{C}_{33}$ of the effective elastic compliance are non-zero. Thus, in this case the axes of principal stress and principal strain do not coincide, and we have non-zero shear strain (Fig. 6(c)) in the coordinate system 102. In the post-failure regime, the number of damage directions does not increase significantly. A single damage continues to grow in the post-failure region. It was found that with increasing confining stress, the damage in planes whose normals are perpendicular to the applied load direction 01 vanishes. In other words, the initiation of crack or damage planes parallel to the load direction decreases with increasing confinement. At zero confining stress ($\sigma_2 = 0$), the active damage plane is inclined at an angle of 12 degrees to the 01 axis and at $\sigma_2 = -10$ MPa, it is inclined at an angle of 15 degrees to the 01 axis.

The results for a numerical experiment in which a body is subjected to unloading and re-loading under compression, for non-conjugate damage growth and under zero confining stress, are shown in Fig. 7. In the post-failure regime, the effective Young's modulus decreases (Fig. 7(a)) and the effective Poisson's ratio increases with increasing damage. It is important to note that in the case of the tension experiment, the effective Poisson's ratio decreases with increasing damage (Fig. 4(b)). Unloading from a damage state and reloading
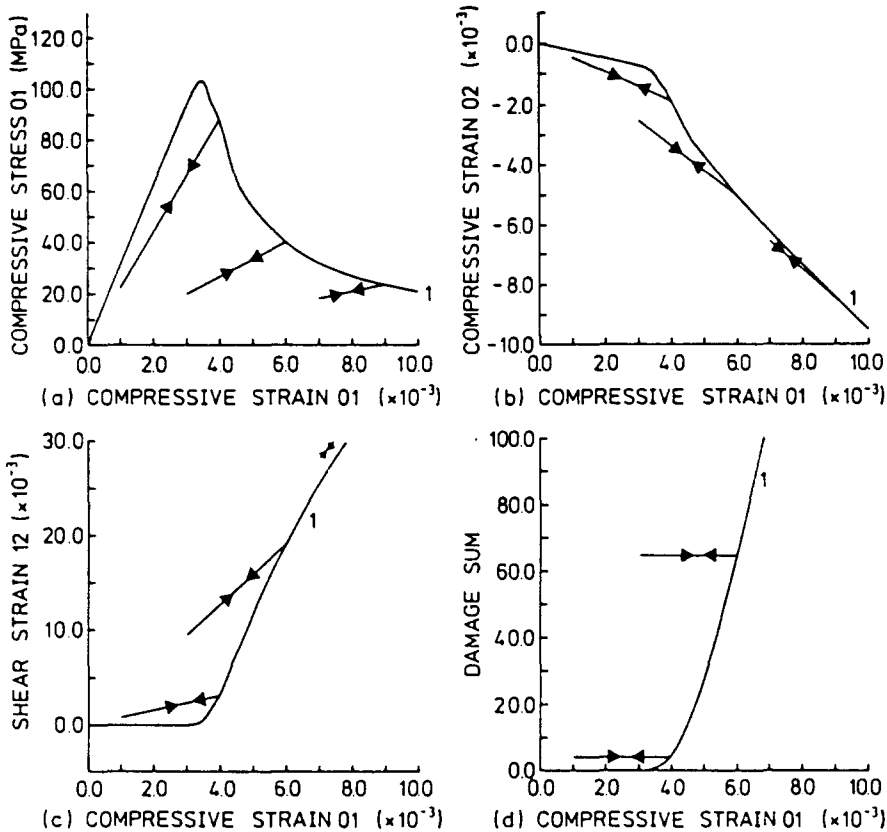
Fig. 7. Numerical compression experiment with non-conjugate damage growth. Curve 1 is unloading-reloading for zero confining stress.

to the same state occurs reversibly (Figs. 7(a), (b), (c)) and at a constant damage level (Fig. 7(d)).

We now summarize the results obtained from the numerical studies of our constitutive model for a body loaded under plane strain conditions as follows.

(i) The compressive strength (the magnitude of the peak compressive load) is about seven times the magnitude of the tensile strength (peak tensile load) (compare the peaks of curve 1 in Fig. 4(a) and curve 1 in Fig. 6(a)). However, a desired strength ratio to be correlated with experimental data for example, may be obtained by adjusting the material parameters.

(ii) The peak-load in tension as well as in compression occurs at a small value of the damage. See Figs 4(d), 5(c) and 6(d). Thus, the normal rock mechanics practice of taking a brittle rock as a "linearly elastic solid" up to the peak-load is justified.

(iii) The effective elastic Poisson's ratio (i.e. the ratio of strain 02 strain 01 on the unloading-reloading part of the curve) decreases in the tension experiment (Fig. 4(b)), and increases in the compression experiment (Fig. 7(b)) with an increase in the damage. The increase in the effective Poisson's ratio under applied compressive loading may explain dilatancy (an increase in the inelastic volume of a specimen) observed in laboratory experiments on brittle rocks (Paterson, 1978).

(iv) Failure in compression (non-conjugate damage growth case) occurs by the growth of a damage plane at a relatively small angle to the applied load direction at low confinement. Failure in tension occurs due to the growth of a damage plane almost normal to the applied load direction.

7. DISCUSSION

Our constitutive model for simulation of progressive failure in brittle rocks is based on the continuum damage mechanics (CDM) approach. Its development does not depend

on any assumption concerning path independence in the small. Discrete phenomena such as the formation and growth of cracks in a brittle rock during the failure process have been characterized in an "average" sense by using a continuum field variable, the so-called "damage" vector. This variable has been used in the formulation of the constitutive relations to describe the development of elastically anisotropic behaviour during the progressive failure process. The damage variable has been taken as an internal variable in the theory of Irreversible Thermodynamics of continua, to derive the constitutive relations (see eqn (9)).

Individual damage surfaces (eqns (12)–(14)) are associated with each damage vector in strain space. There may be many damage vectors at a given point. It is supposed that the damage growth in a given direction is independent of the damage growth in other directions. This assumption could of course be critical in certain cases where our model is used in finite element simulations. We do not yet know how this difficulty could be circumvented. Nevertheless, we have found (Singh and Digby, 1988) that our constitutive model does simulate many of the essential observed features of the progressive failure of a number of brittle rock structures. We define the damage direction uniquely requiring that the damage surface function, $F(\varepsilon)$ (see eqn (13)), is a maximum and a trial strain state lies outside the damage surface (see inequality (16)). Our constitutive model can then describe damage growth in other directions whenever this is required, for example during non-proportional loading and in elastically anisotropic behaviour.

The effective elastic properties of a brittle solid containing "open" flat cracks when the body is loaded under tension differ from those obtained for the same body when it is loaded under compression (in the case of partially or completely closed cracks), since in the latter case, the question of crack closure must be considered. The effective Young's modulus of elasticity in both cases is less than the initial Young's modulus for the uncracked material. The effective Poisson's ratio of a solid containing very flat *open cracks* is less than the initial Poisson's ratio, and the effective Poisson's ratio of a solid containing *closed cracks* is greater than the Poisson's ratio for the uncracked body (see Jaeger and Cook, 1979, p. 336). In our formulation of the effective compliance of a rock containing cracks (eqn (30)), we have considered also the question of crack closure. The compressive crack closure stress, σ_{y_c} plays a vital role in the behaviour of our constitutive model for a body loaded in compression. If the magnitude of σ_{y_c} is too large, then under an applied uniaxial compressive stress, all flat cracks will remain open, even in the post-failure region. The behaviour of the rock considered will not then be simulated correctly. We have therefore selected a small value of σ_{y_c} (= −0.5 MPa) applicable to a very flat crack.

From our numerical simulations it will be noticed that we have not performed a series of material parametric ("sensitivity") studies for a range of materials under given loading conditions. It can be seen from the earlier sections of this paper that equally large or even far greater contrasts in the constitutive behaviour of a cracked solid may be observed by studying a given cracked solid under different applied loading conditions. A numerical study of the post-failure behaviour of an infinitely extended cracked brittle solid loaded under a number of plane strain loading conditions was therefore studied. Since the body considered is infinitely extended, we suppose that the damage in any direction is uniformly distributed throughout the body, and further, therefore, that localization effects need not be considered for this group of idealized problems. In a companion paper (Singh and Digby, 1989) we will consider finitely extended bodies and localization effects will be considered in detail. Here, our constitutive model will be generalized in such a manner that the damage growth model for localized elements differs from our original one used for those elements which have not localized. We shall also demonstrate the application of our constitutive model by performing a number of finite element analyses of some brittle rock structures which might actually be encountered in underground structures.

REFERENCES

Davison, L. and Stevens, A. L. (1973). Thermomechanical constitution of spalling elastic bodies. *J. Appl. Phys.* **44**, 668.
Digby, P. J. and Murrell, S. A. F. (1976). The deformation of flat ellipsoidal cavities under large confining pressures. *Bull. Seismol. Soc. Am.* **66**, 425.

Dougill, J. W. (1975). Some remarks on path independence in the small in plasticity. *Q. Appl. Math.* **33**, 233.

Dragon, A. and Mroz, Z. (1979). A continuum model for plastic-brittle behaviour of rock and concrete. *Int. J. Engng Sci.* **17**, 121.

Grady, D. E. and Kipp, M. E. (1980). Continuum modelling of explosive fracture in oil shale. *Int. J. Rock Mech. Min. Sci. Geomech. Abstr.* **17**, 147.

Horii, H. and Nemat-Nasser, S. (1983). Overall moduli of solids with microcracks: load-induced anisotropy. *J. Mech. Phys. Solids* **31**, 155.

Jaeger, J. C. and Cook, N. G. W. (1979). *Fundamentals of Rock Mechanics*, 3rd edn. Chapman and Hall, London.

Kachanov, M. L. (1958). Time of the rupture process under creep conditions. *Isv. Akad. Nauk S.S.R. Otd. Tekh.* **8**.

Kestin, J. and Bataille, J. (1977). Irreversible thermodynamics of continua and internal variables. In *Continuum Models of Discrete Systems*. (Edited by J. W. Provan). p. 39. University of Waterloo Press.

Krajcinovic, D. and Fonseka, G. U. (1981). The continuous damage theory of brittle materials. Part I: General theory. *J. Appl. Mech.* **48**, 809.

Lama, R. D. and Vutukuri, V. S. (1978). *Hand Book on Mechanical Properties of Rocks*, Vol. II. Trans. Tech. Publications, Clausthal.

Lemaitre, J. (1986). Local approach of fracture. *Engng Fract. Mech.* **25**, 523.

Murrell, S. A. F. and Digby, P. J. (1970). The theory of brittle fracture initiation under triaxial stress conditions—I. *Geophys. J. R. Astr. Soc.* **19**, 309.

Paterson, M. S. (1978). *Experimental Rock Deformation—the Brittle Field*. Springer, Berlin.

Resende, L. and Martin, J. B. (1984). A progressive damage 'continuum' model for granular materials. *Comput. Meth. Appl. Mech. Engng* **42**, 1.

Rice, J. R. (1971). Inelastic constitutive relations for solids: an internal variable theory and its application to metal plasticity. *J. Mech. Phys. Solids* **19**, 433.

Rice, J. R. (1975). Continuum mechanics and thermodynamics of plasticity in relation to microscale deformation mechanisms. In *Constitutive Equations in Plasticity*. (Edited by A. S. Argon), p. 23. The MIT Press, Cambridge.

Shahidi, P., Stephansson, O. and Singh, U. K. (1986). Control of uniaxial tension and simple shear test after peak-load. Research Report TULEA 1986: 15, Luleå University, Sweden.

Singh, U. K. and Digby, P. J. (1989). The finite element simulation of the progressive failure of a brittle rock. *Int. J. Solids Structures* (accepted for publication).

Singh, U. K. (1986). Simulation of strain softening behaviour of brittle rock: a continuum damage mechanics approach. Licentiate thesis 1986: 002L, Luleå University, Sweden. Work also published as: Singh, U. K., Digby, P. J. and Stephansson, O. J. (1987). Constitutive equation for progressive failure of brittle rock. In *Constitutive Laws for Engineering Materials: Theory and Applications*, Vol. II. (Edited by C. S. Desai, E. Krempl, P. D. Kiousis and T. Kundu), pp. 923–930. Elsevier, London.

Walsh, J. B. (1965). The effect of cracks on the compressibility of rock. *J. Geophys. Res.* **70**, 381. Cited by Digby and Murrell (1976).